

1 Electronic Supporting Information (ESI):
2 Ensemble based screening of natural products and FDA
3 approved drugs identified potent inhibitor of SARS-CoV-2
4 that work by two distinct mechanisms

5 Daniel M Shadrack^{1,2*}, Geradius Deogratias^{3,4}, Lucy W Kiruri⁵, Hulda S
6 Swai¹, John-Mary Vianney¹, Stephen S Nyandoro^{3*}

7 ¹Department of Health and Biomedical Sciences, School of Life Science and Bioengineering, The
8 Nelson Mandela African Institution of Science and Technology, P.O.Box 447, Arusha, Tanzania.

9 ²Department of Chemistry, Faculty of Natural and Applied Sciences, St John's University of
10 Tanzania, P.O.Box 47, Dodoma, Tanzania

11 ³Chemistry Department, College of Natural and Applied Sciences, University of Dar es Salaam, P.O.
12 Box 35061, Dar es Salaam, Tanzania

13 ⁴Department of Materials and Energy Science and Engineering, The Nelson Mandela African
14 Institution of Science and Technology, P.O.Box 447, Arusha, Tanzania.

15 ⁵Department of Chemistry, Kenyatta University, Nairobi, Kenya

16 **Table S1.**

17 As described in the main text, two validation approaches were used to validate the docking
18 algorithm used in this work. A comparison to experimental binding free energy obtained from
19 literature (Baum et al., 2009 & Baum et al., 2010) were used as described in the main text.

Table S1: Comparison of experimental binding free energy and calculated free energy (kcal/mol). A reasonable agreement was obtained with $r^2=0.83$.

PDB ID	ΔG_{Exp}	ΔG_{Cal}
2ZFP	-7.48	-7.9
2ZGB	-8.38	-8.3
2ZC9	-8.46	-9.7
2ZI2	-7.83	-8.6
2ZIQ	-8.93	-9.4
2ZHQ	-9.03	-9.8
2ZDA	-11.01	-10.3

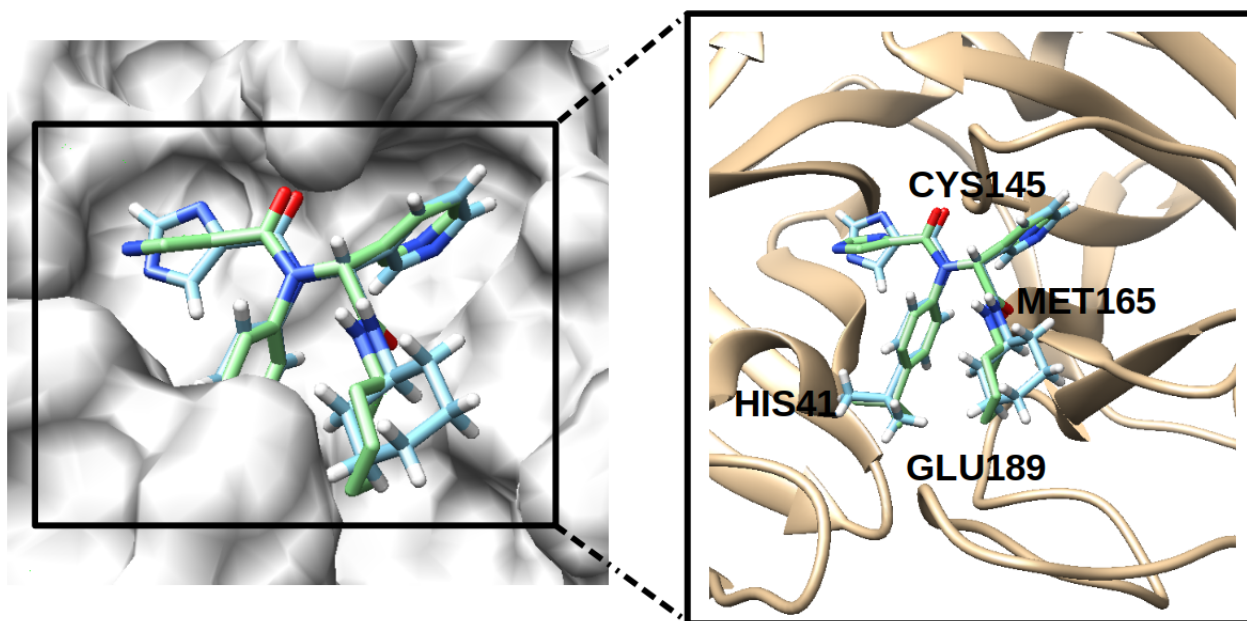


Figure S1: Validation of docking methods. Redocking of a ligand 3CLpro (6W63) gave an RMSD value of 2.5 Å. Light blue is the crystal structure, light green is the redocked structure.

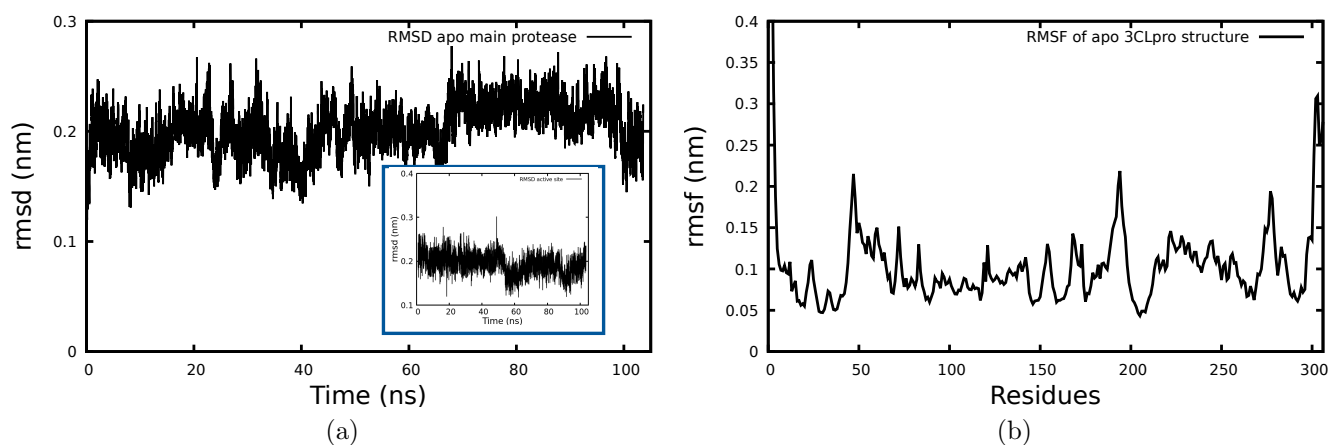


Figure S2: (a) RMSD and (b) RMSF of apo 3CLpro. An insert shows the active site RMSD. RMSF shows only few fluctuation at the region made up of the loops.

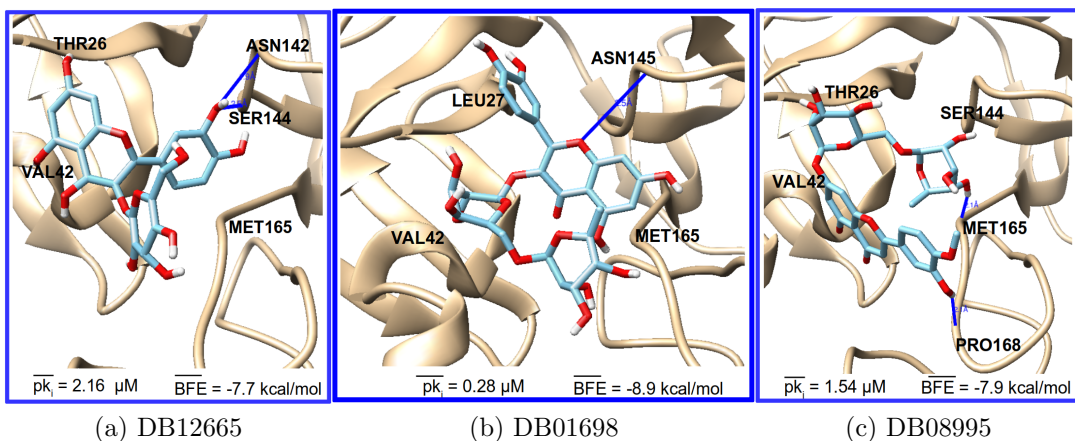


Figure S3: Binding free energy and binding modes of three screened drug hits against SARS-CoV-2 target.

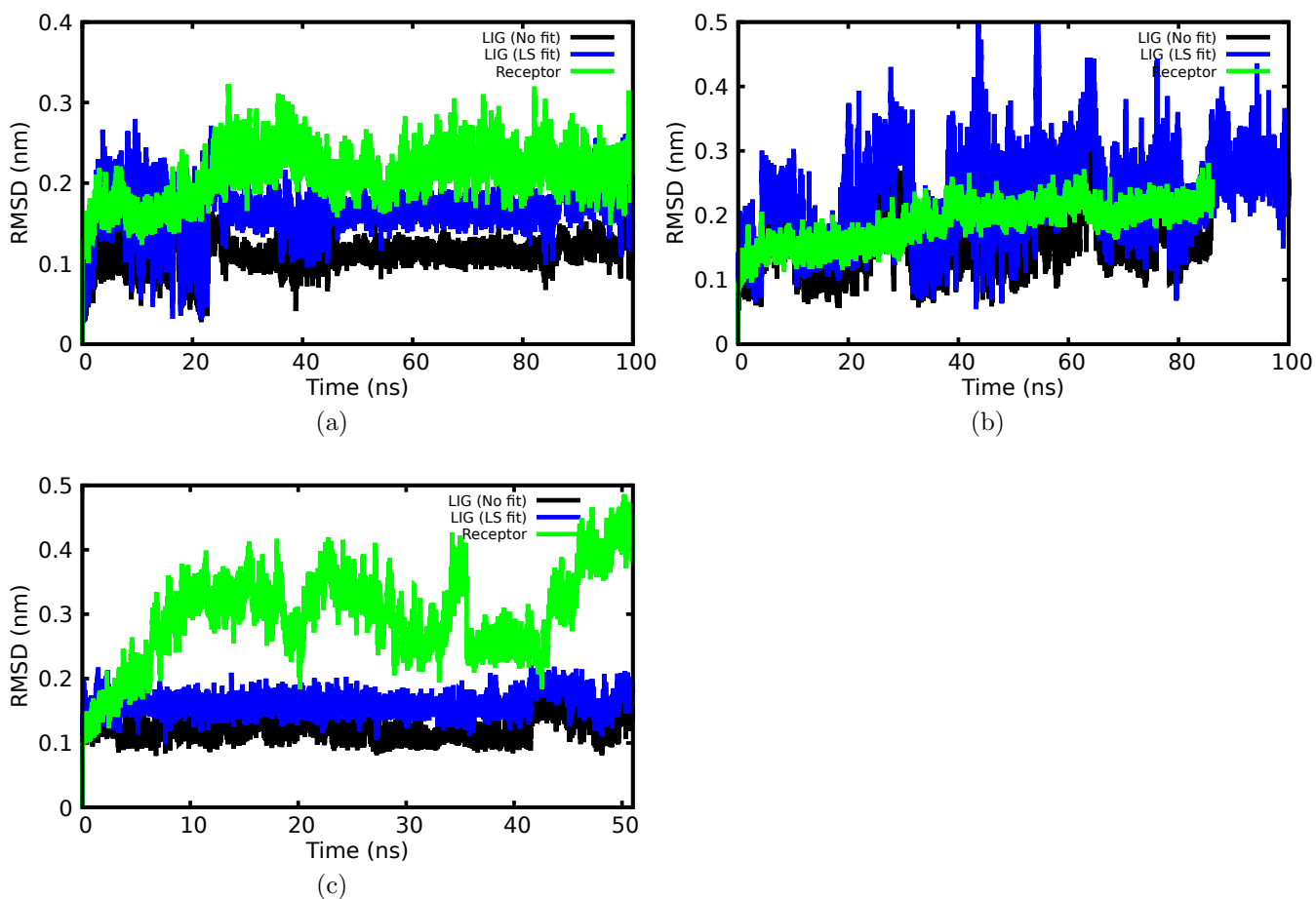


Figure S4: (a) RMSD of complex and ligand over the simulation time.

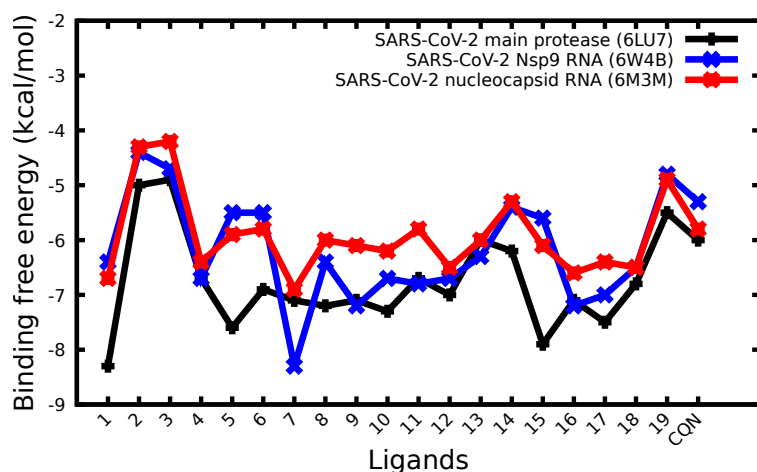


Figure S5: Screening of in-house library against 3CLpro, nucleocapsid NRA and Nsp9 RNA.

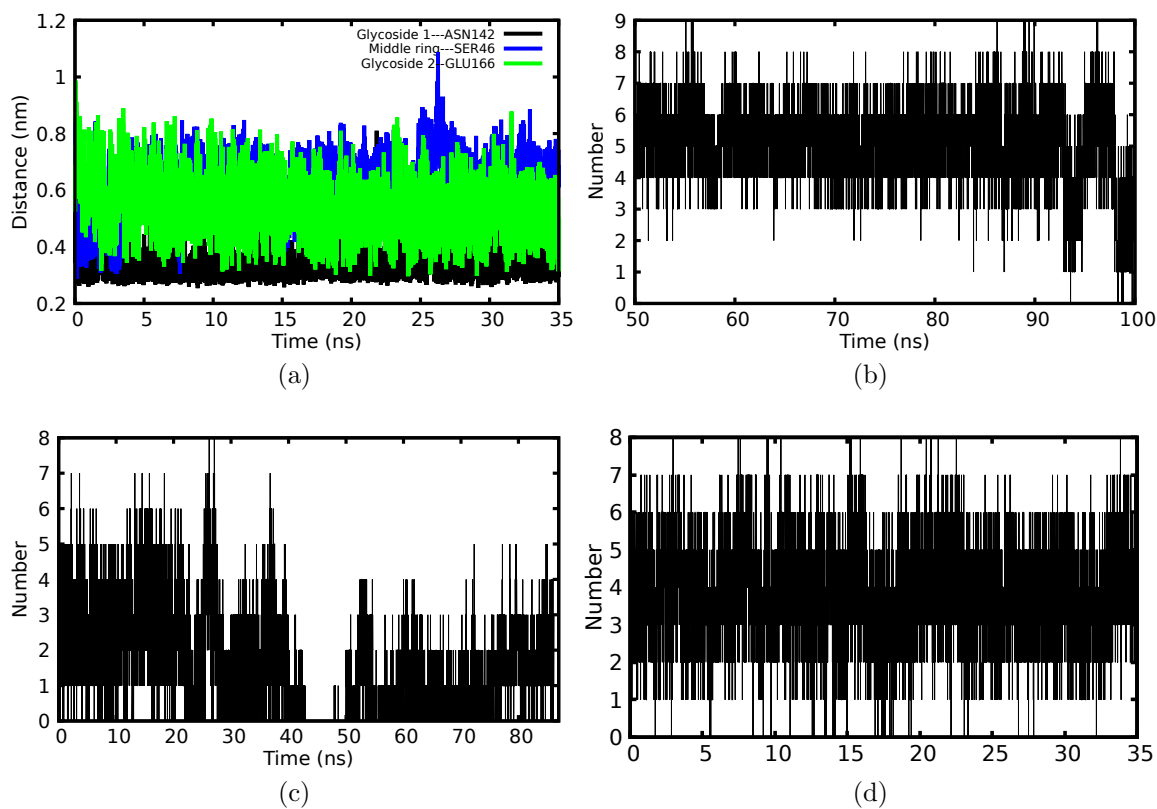


Figure S6: (a) H-bond distances between protein and groups of DB08995, b-d number of hydrogen bonds formed between drugs and 3CLpro. (b) DB12665, (c) DB01698 and (d) DB08995.

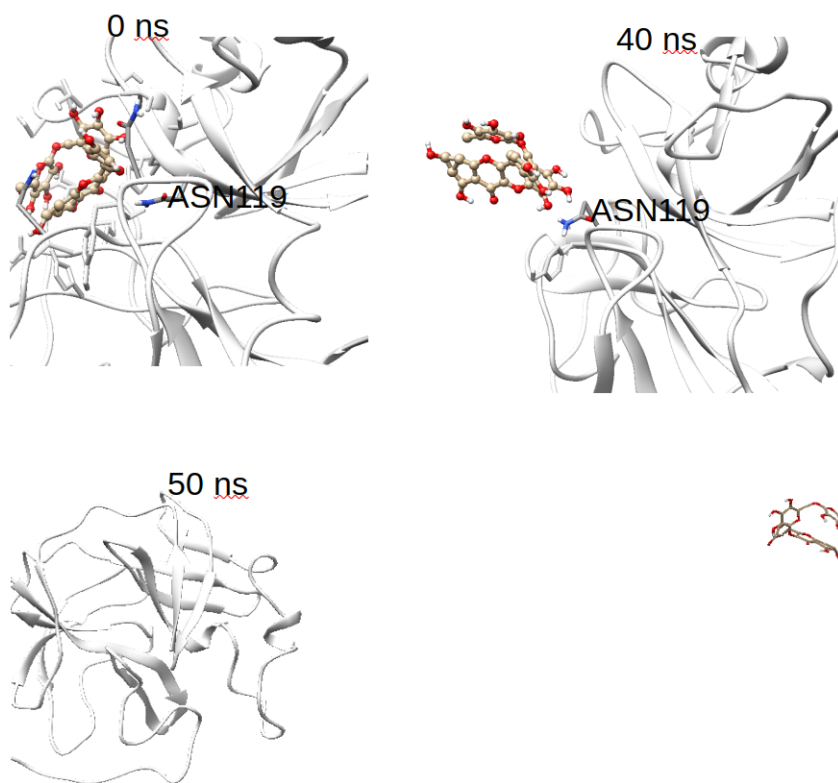


Figure S7: Interaction between ligand DB01698 and Mpro, suggesting that ligand moved out of the pocket as shown during the 50 ns.

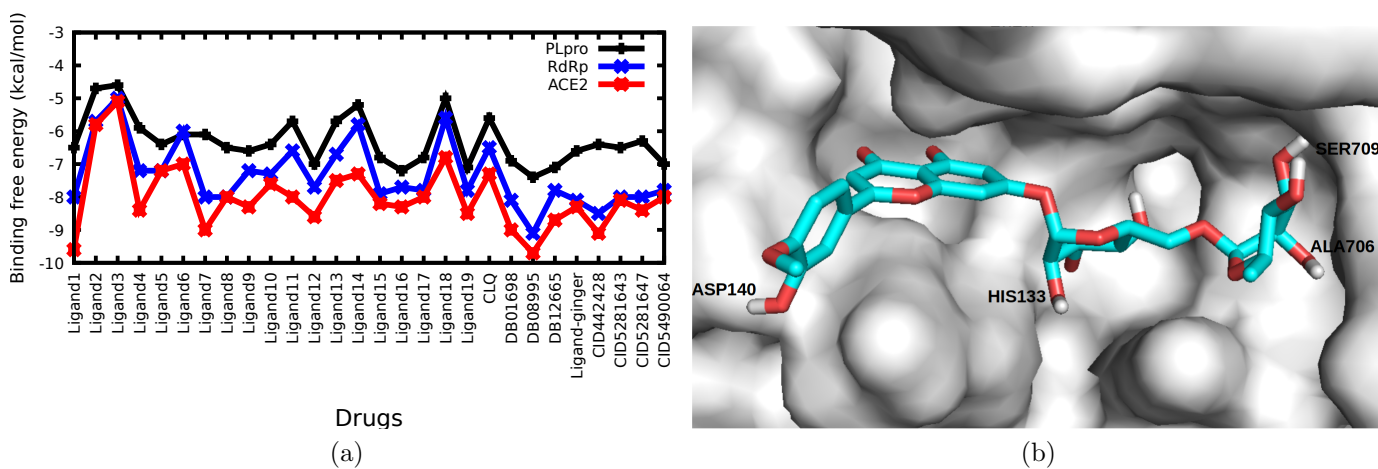


Figure S8: (a) Binding free energy of ligands to three SARS-CoV-2 target (b) Binding mode of DB08995 into RdRp pocket.

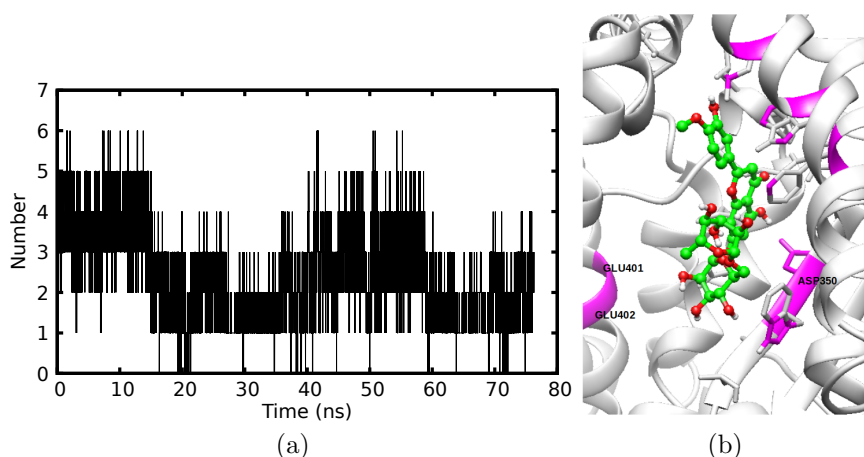


Figure S9: Interactions of DB08995 with ACE2 target during MD simulation. (a) number of hydrogen bonds formed (b) binding pose of DB08995 inside ACE2 active site showing important residues responsible for the interaction.

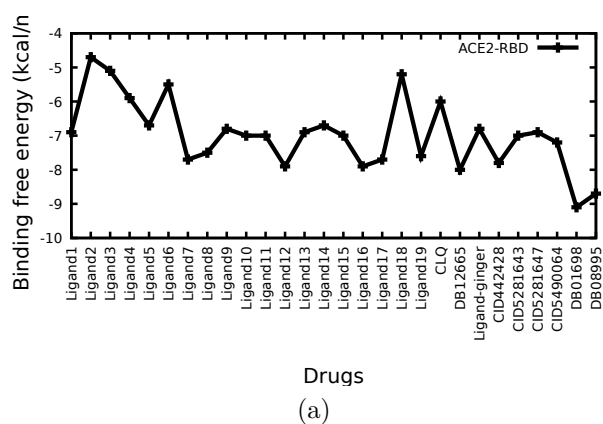


Figure S10: targeting inhibition of ACE2-RBD

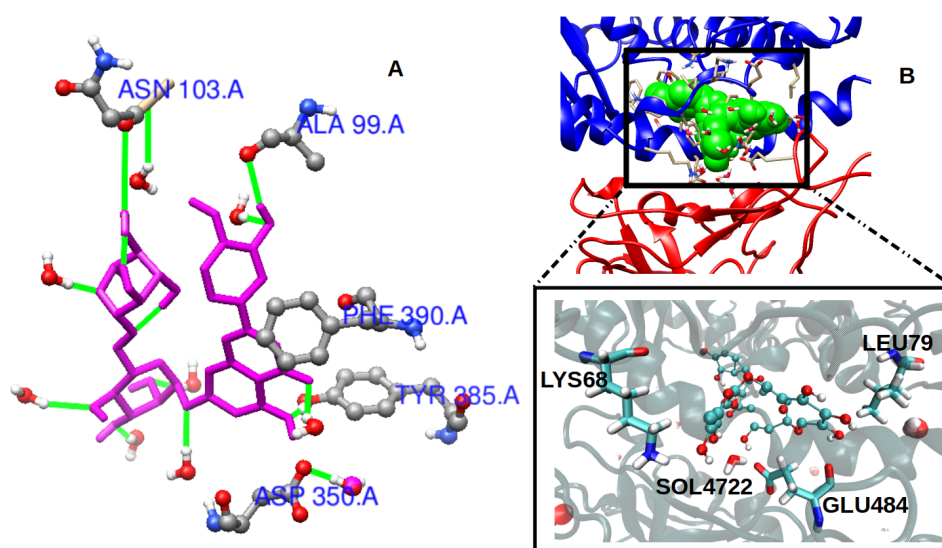


Figure S11: Water mediated the interaction between DB08995 and the spike RBD-ACE by forming hydrogen bonds. Right panel is the interaction of water with both DB08995 in the putative ACE2 active site and left panel is the interaction of water with both spike RBD and ACE2.

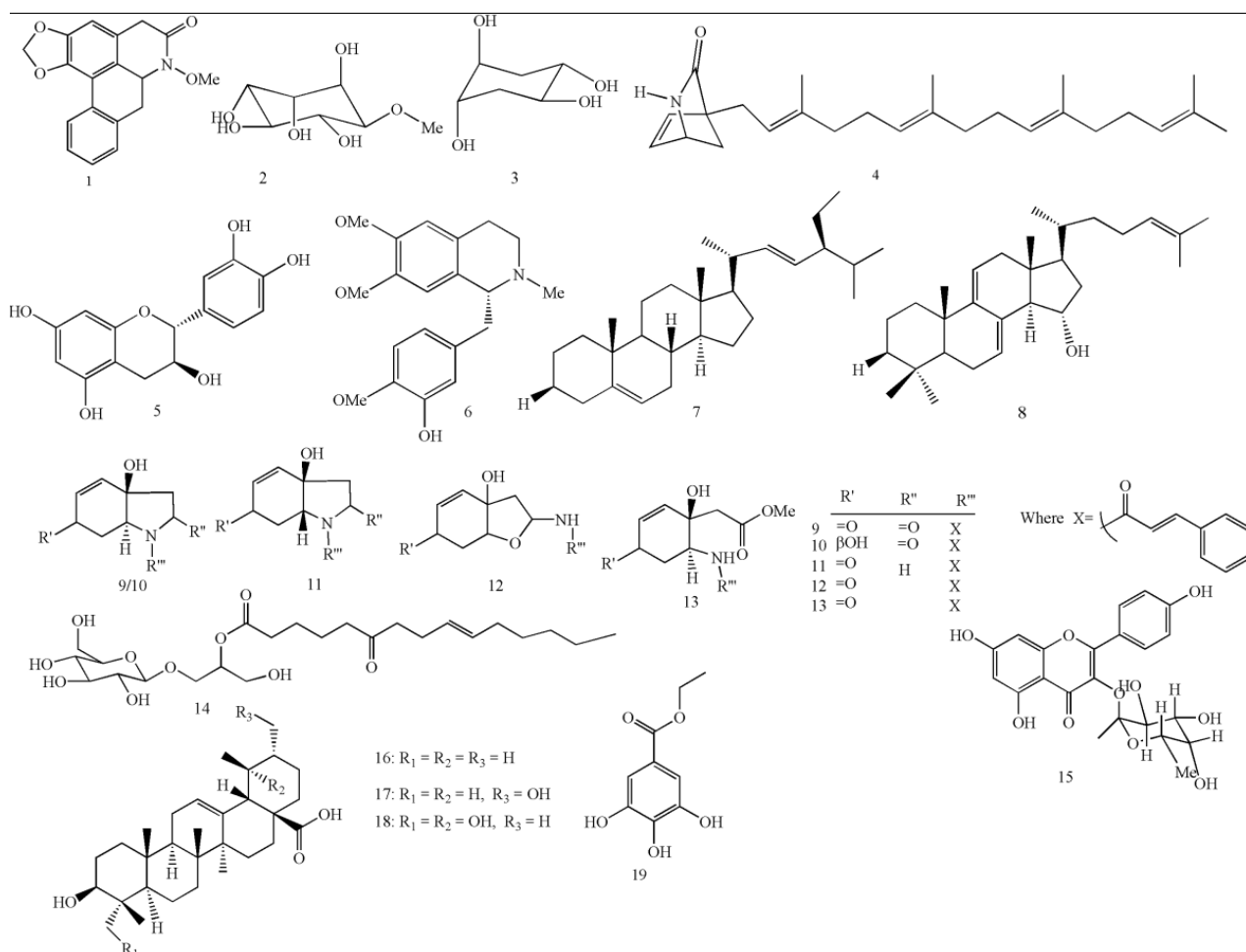


Figure S12: Natural products from our library